JACS
JOURNAL OF THE AMERICAN CHEMICAL SOCIETY
Communication
pubs.acs.org/JACS

Catalytic and Biocatalytic Iron Porphyrin Carbene Formation: Effects of Binding Mode, Carbene Substituent, Porphyrin Substituent, and Protein Axial Ligand

Rahul L. Khade and Yong Zhang*

Department of Chemistry, Chemical Biology, and Biomedical Engineering, Stevens Institute of Technology, Castle Point on Hudson, Hoboken, New Jersey 07030, United States

Supporting Information

ABSTRACT: Iron porphyrin carbenes (IPCs) are important intermediates in various chemical reactions catalyzed by iron porphyrins and engineered heme proteins, as well as in the metabolism of various xenobiotics by cytochrome P450. However, there are no prior theoretical reports to help understand their formation mechanisms and identify key information governing the binding mode, formation feasibility, and stability/reactivity. A systematic quantum chemical study was performed to investigate the effects of carbene substituent, porphyrin substituent, and axial ligand on IPC formation pathways. Results not only are consistent with available experimental data but also provide a number of unprecedented insights into electronic, steric, and H-bonding effects of various structural factors on IPC formation mechanisms. These results shall facilitate research on IPC and related systems for sustainable chemical catalysis and biocatalysis.

The excellent catalytic performance of P450 cytochromes for numerous biochemical reactions[1] has spurred extensive efforts in developing biomimetic metalloporphyrin catalysts for carbene transfers in a broad range of organic reactions including C−H insertion, N−H insertion, cyclopropanation, as well as the olefination of aldehydes and ketones.[2−30] The key active species have been proposed to be metalloporphyrin carbenes. In particular, iron porphyrin carbenes (IPCs) implied in many studies[4,15,18,21−25] have been directly shown to undergo several of these chemical reactions, including C−H insertions and cyclopropanations.[13] IPC complexes were first observed several decades ago in the reactions of polyhalogenated methanes with porphyrins,[31] reactions similar to those observed in the metabolism by cytochrome P450 of xenobiotics.[32] More recently, various engineered heme proteins such as cytochrome P450, horseradish peroxidase, cytochrome *c*, and myoglobin were used for the catalysis of carbene transfer with excellent reactivity and selectivity.[33] IPCs were also assumed as key intermediates in such biocatalytic reactions.

However, the IPC formation mechanism and specific factors governing IPCs' binding mode, formation feasibility, and stability/reactivity have not been reported. Such kind of information is critical to help understand their catalytic performance, especially since the carbene formation from the diazo precursors with metal complexes was found to be basically the rate-determining step in several reactions catalyzed by iron porphyrin and other metal catalysts.[9,15,34] Therefore, a systematic quantum chemical investigation was performed here to reveal the first detailed IPC formation pathways as well as the first theoretical insights into effects of binding mode, carbene substituent, porphyrin substituent, and protein axial ligand on IPC formation. Results will facilitate mechanism-based design of useful carbene transfer catalysts and biocatalysts.

Scheme 1. IPC Formation Pathway (Ovals Represent Porphyrin)

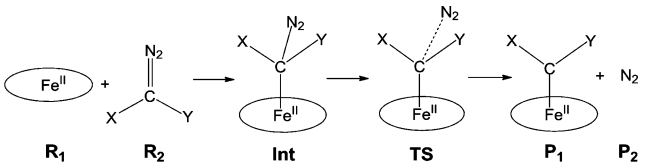

One of the first isolated IPC complexes that can perform C−H insertions of unfunctionalized alkenes,[13] Fe(TPFPP)(C(Ph)-CO_2Et) (**1**, TPFPP = *meso*-tetrakis(pentafluorophenyl)-porphyrinato dianion) was taken as an example to reveal the basic IPC formation pathway. TPFPP was modeled as a nonsubstituted porphyrin (Por). All species were subject to full geometry optimization and frequency analysis in the solvent used experimentally,[13] using a range-separated hybrid DFT method with dispersion correction, ωB97XD,[35] based on its previous excellent performance on other systems in catalysis[36] and NMR shift predictions of IPCs,[37] and a methodological study in this work (see Supporting Information (SI)). Scheme 1 shows that the basic IPC formation pathway from an Fe^{II}(Por) (**R$_1$**) and a diazo compound (**R$_2$**) proceeds first to form a carbon-coordinated intermediate (**Int**) and then undergoes a transition state (**TS**) to yield the ferrous IPC[37] (**P$_1$**) and N_2 (**P$_2$**). Interestingly, results from the current work using various methods (see SI) provide the first theoretical evidence that the most favorable spin states for **Int** and **TS** in the IPC formation pathway are low spin, similar to those in the metallocarbene formation pathways for dirhodium catalyst,[34] even though the starting Fe^{II}(Por) is triplet. As shown in Table 1, the moderate Gibbs free energy of activation ($\Delta G^{\ddagger}$) of 15.84 kcal/mol and large negative free energy of reaction (ΔG°) of −17.45 kcal/mol

Received: April 1, 2015
Published: June 11, 2015

DOI: 10.1021/jacs.5b03437
J. Am. Chem. Soc. 2015, 137, 7560−7563

Table 1. Key Energetic, Charge, and Geometric Results[a]

	$\Delta G^{\ddagger}$ (kcal/mol)	$\Delta G°$ (kcal/mol)	ΔQ_{Fe} (*e*)	ΔQ_{C} (*e*)	Q_{CT} (*e*)	ΔR_{CN} (Å)	R_{FeC}^{TS} (Å)
1	15.84	-17.45	-0.485	0.150	-0.326	0.469	1.966
2	21.94	0.81	-0.222	0.185	-0.248	0.635	2.225
3	13.72	-11.78	-0.556	0.208	-0.372	0.496	1.882
4	18.19	-23.51	-0.434	0.079	-0.327	0.429	2.048
5	9.88	-18.51	-0.521	0.122	-0.388	0.450	1.921
6	6.69	-23.81	-0.501	0.165	-0.344	0.498	1.976
7	27.18	-7.84	-0.481	0.142	-0.308	0.455	1.960
8	13.59	-20.41	-0.479	0.154	-0.327	0.470	1.963
9	27.84	-9.36	-0.816	0.080	-0.254	0.489	2.167
10	43.59	2.03	-0.742	0.083	-0.190	0.495	2.178
11	21.61	0.61	-0.961	0.205	-0.314	0.546	1.936
12	36.96	12.80	-0.863	0.173	-0.231	0.511	1.941

[a]Changes are those at **TS** with respect to reactants. Compound names: **1**, Fe(Por)(C(Ph)CO_2Et); **2**, Fe(Por)(C(Ph)CO_2Et)$_2$; **3**, Fe(Por)(CHCO_2Et); **4**, Fe(Por)(CPh_2); **5**, Fe(Por)(CHPh); **6**, Fe(Por-4-*meso*-NO_2)(CPh(CO_2Et)); **7**, Fe(Por-4-*meso*-NH_2)(CPh(CO_2Et)); **8**, Fe(Por-*meso*-HBG)(CPh(CO_2Et)), see Figure 2B for HBG identity; **9**, Fe(Por)(CPh_2)(MeIm); **10**, Fe(Por)(CPh_2)(SH^-); **11**, Fe(Por)(CHCO_2Et)(5-MeIm); **12**, Fe(Por)(CHCO_2Et)(SH^-); see SI for optimized structures.

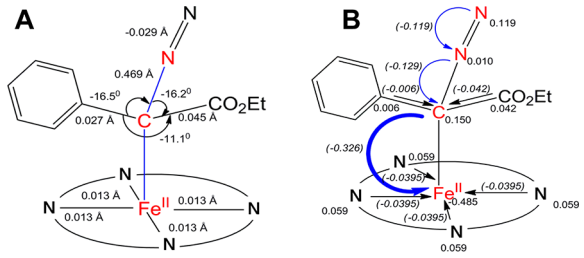

Figure 1. Key bond length and bond angle changes (A) and atomic charge changes (B) (unit: *e*) from reactants to **TS**. Charge transfers are indicated by arrows and numbers in parentheses in (B).

are consistent with the facile experimental room-temperature synthetic result.[13]

To help reveal key structural changes and major electronic driving force in this pathway, both geometric data and charge profiles were examined in detail (see SI) with key results shown in Figure 1. The largest bond length change from reactants to **TS** occurs with the partially broken bond C−N (in blue), an elongation of 0.469 Å, in addition to the partially formed new Fe−C bond in **TS** with R_{FeC}^{TS} = 1.966 Å. The decrease of 11−16° for bond angles around the carbene center indicates the geometric change of the planar conformation in $\mathbf{R_2}$ to a basically tetrahedral configuration in the **TS**. Consistent with these geometric changes, the largest atomic charge changes were found to be with Fe (−0.485 *e*) and C (0.150 *e*) (Table 1, Figure 1). Large charge transfer (CT) occurs from the N_2 moiety to carbene carbon, which along with minor charge donation from carbene substituents, constitute a significant CT of Q_{CT} = −0.326 *e* from carbene to iron. As a result, the carbene carbon bears a partial positive charge in the final product as reported recently,[37] ready for subsequent electrophilic reactions.[13,15,21,22] These results for the first time show that, the major electronic driving force here is the CT from the carbene carbon to the metal center, offering a general mechanism to understand various structural factors on IPC formation (*vide infra*).

It should be noted that in the above studies, the formed IPC complex has a Fe−C terminal binding mode, which is the same as found in all available experimental Fe^{II}(Por) carbene X-ray structures.[13,38] However, it is still unclear why the bridging binding mode which involves bonding with both Fe and porphyrin nitrogen to carbene carbon (see SI, Figure S2, right panel) has not been reported, although for Co^{II}(Por) carbenes, the bridging mode was found to be actually energetically more favorable than the terminal binding mode.[9] Our calculations show that the bridging binding mode for **1** is 13.17 kcal/mol higher energy than the terminal mode, in contrast with ca. −2 kcal/mol in the case of Co^{II} systems. This large energy preference offers an excellent explanation of the experimentally exclusive finding of terminal binding modes in isolated IPC complexes. To help further understand the electronic origin of this preference, the frontier MOs containing iron 3d orbitals were examined for both binding modes. The key difference was found with the relative order of d_{z^2} and d_{yz} (see Figure S2). The terminal binding mode of **1** has the same order as reported recently for other terminal bound IPCs:[37] d_{z^2} is unoccupied while d_{yz} is occupied, since in the terminal binding mode the repulsion between carbene and d_{z^2} is larger than that with d_{yz}. However, in the bridging binding mode, the carbene ligand is shifted away from d_{z^2} direction and is more closely aligned toward d_{yz}, and thus its repulsion with d_{yz} is stronger than that with d_{z^2}, which results in the reverse of these two d orbital order. Additional calculations were done to help understand, why no biscarbene iron porphyrins have been reported while Os, the late transition metal in the same group of Fe, can form the biscarbene species as the active catalyst.[17] As shown in Table 1, regarding key parameters for the IPC formation profiles for Fe(Por)(C(Ph)-CO_2Et)$_2$ (**2**) using the monocarbene species **1** as $\mathbf{R_1}$, $\Delta G^{\ddagger}$ is increased by ∼6 kcal/mol, and $\Delta G°$ is significantly increased by ∼18 kcal/mol to result in thermodynamically unfavorable formation. This is probably due to the *trans* effect of carbene ligand, which makes the second carbene more weakly bound to Fe. In fact, an increase of 0.259 Å in R_{FeC}^{TS} for **2** compared to the monocarbene **1** was found (see Table 1 for the data of the second carbene). Accordingly, a stable **Int** for this biscarbene formation was not found. These results provide the first theoretical insights into experimental data that the ferrous IPC complex prefers the terminal, monocarbene mode, which will be used in the following studies of various structural factors on IPC formation profiles to reveal useful molecular design guidelines for IPC catalysts.

We first investigated carbene substituent effect. Since ethyl diazoacetate (EDA) is frequently used in carbene-transfer reactions with metalloporphyrin and heme protein catalysts,[9,10,13,20−24,26,27,33a,c−e] the IPC formation pathway for Fe(Por)-(CHCO_2Et) (**3**) was studied. As shown in Table 1, compared to *α*-phenyl-substituted **1**, $\Delta G^{\ddagger}$ of **3** reduces by 2.12 kcal/mol and $\Delta G°$ increases by 5.67 kcal/mol, albeit still thermodynamically favorable. Both the relatively lower barrier and higher product energy help the facile formation of a more reactive **3** compared to **1**, which is consistent with experimental report.[13] The relatively higher $\Delta G^{\ddagger}$ of **1** vs **3** is probably due to the steric effect of *α*-phenyl substituent, as evidenced by ∼5° larger bond angle of the two carbene substituents in **1** throughout $\mathbf{R_2}$, **Int**, and **TS**, and correspondingly 0.084 Å longer R_{FeC}^{TS}. The $\Delta G^{\ddagger}$ of Fe(Por)-(CPh_2) (**4**) with two phenyl substituents was calculated to be almost double of that of Fe(Por)(CHPh) (**5**) (Table 1). These results provide the first computational evidence that bulky substituent on carbene hinders IPC formation and subsequent reactivity, but stabilizes IPC for isolation and characterization, which is in good accordance with experimental results.[13] Comparing data for the less steric IPCs **3** and **5** clearly shows that, regarding electronic effects, the more electron-donating

DOI: 10.1021/jacs.5b03437
J. Am. Chem. Soc. 2015, 137, 7560−7563

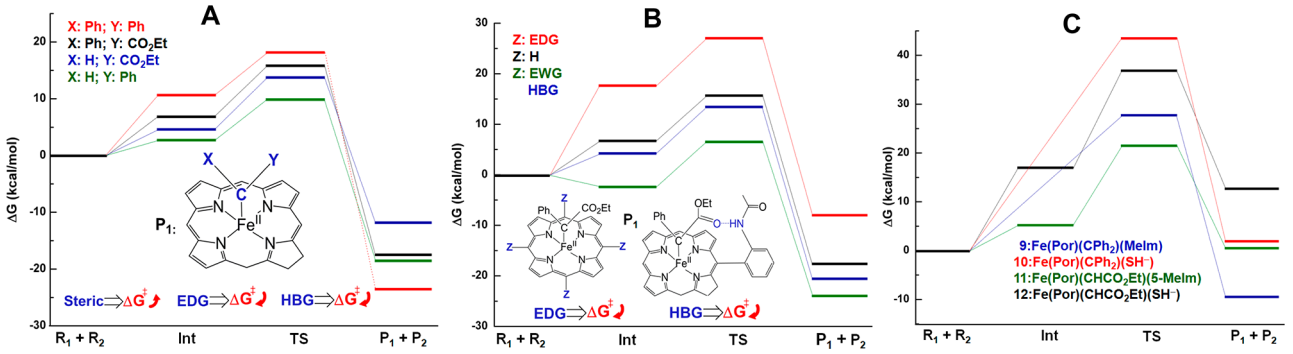

Figure 2. Effects of (A) carbene substituent, (B) porphyrin substituent, and (C) axial ligand on IPC formation.

group (EDG) Ph in **5** vs the electron-withdrawing group (EWG) CO_2Et in **3** results in a more favorable reaction barrier. This is consistent with the IPC formation mechanism and electronic driving force described in Figure 1; i.e., EDG on carbene helps charge donation from carbene to iron than EWG to facilitate the IPC formation, as evidenced by the enhanced Q_{CT} by −0.016 *e*. However, for Fe(Por)(CPh(X)), the barrier for X = CO_2Et in **1** is lower than that for X = Ph in **4**, which does not follow the simple electronic effect. Nevertheless, a H-bond between phenyl H and carbonyl O in **TS** for **1** was found, with H···O distance of 2.226 Å, which helps stabilize this **TS** and thus lowers the barrier. The reduction in $\Delta G^{\ddagger}$ of 2.35 kcal/mol here is similar to that from the H-bonding effect, $\Delta G^{\ddagger}$ reduction of 3.1 kcal/mol, in Co^{II}(Por).[9] The mildly more favorable barrier for **1** vs **4** together with the more significantly less favorable reaction energy could result in similar yields of these two IPCs, as observed experimentally.[13] Overall, these results clearly indicate that the steric effect, electronic effect, and H-bonding capability can play important roles on IPC formation, as summarized in Figure 2A.

Besides carbene substituent, porphyrin substituent has also been found to have important effects on metalloporphyrin carbene stabilities/reactivities.[2] In particular, experimental studies suggest that the electron-deficient nature of the pentafluorophenyl substituent on porphyrin *meso* positions help stabilize the resultant IPC, in contrast with the non-fluorinated phenyl substituent on the same positions.[13] This can be explained by using the IPC formation mechanism described above, since porphyrin with EWG can help promote CT (the electronic driving force here) from carbene carbon to the metal center, and, thus, would bring down the barrier and reaction energy. To verify this, the formation pathways for Fe(Por-4-*meso*-NO_2)(CPh(CO_2Et)) (**6**) and Fe(Por-4-*meso*-NH_2)(CPh-(CO_2Et)) (**7**) were investigated, with strong EWG and EDG on four porphyrin *meso* positions, respectively. As shown in Table 1 and Figure 2B, the use of EWG indeed significantly reduces both $\Delta G^{\ddagger}$ and ΔG°, while EDG has an opposite effect on both kinetic and thermodynamic trends. The effect on Q_{CT} is also obvious and consistent with the described mechanism; i.e., EWG improves it by 0.018 *e*, while EDG reduces it by 0.018 *e*. The use of one hydrogen-bonding group (HBG) as shown in Figure 2B on the IPC formation of Fe(Por-*meso*-HBG)(CPh(CO_2Et)) (**8**) was also studied. This group was previously found to facilitate carbene formation and stabilization in Co^{II}(Por).[9] As seen from Table 1 and Figure 2B, this HBG was found to also stabilize the formed carbene and yields $\Delta G^{\ddagger}$ reduction of 2.25 kcal/mol, similar to the observed H-bonding effect studied above for the carbene substituent. It is interesting to note that HBG basically does not affect Q_{CT} (Table 1) and thus offers an additional approach to regulate IPC formation. These results clearly suggest that the porphyrin substituent, which can facilitate carbene-to-metal CT and/or stabilization of carbene substituent, may be employed to enhance IPC formation and stabilization.

The axial ligand is another tunable part of heme proteins and metalloporphyrins, which has been found to play significant roles on regulating catalytic reactivities.[2] In fact, the heme protein active site and in particular the axial ligand affects carbene transfer and selectivity.[33a] For instance, the Ser-substituted cytochrome P450 is more efficient than its native axial Cys ligand in catalyzing carbene transfer,[33b] and the His-ligated P450 is even better.[33d] In particular, the mutated myoglobin with His ligand catalyzed cyclopropanations with excellent yields (up to 99%) and diastereo- and enantioselectivity (up to 98−99.9%).[33c] Regarding heme model systems, the use of *N*-methylimidazole (MeIm) as an axial ligand to Fe(TPFPP)(CPh_2) was found to improve its reactivity.[13] However, it is still unknown how the axial ligand affects IPC formation. So, here the IPC formation profiles for MeIm and SH^- ligands were investigated. The experimentally used MeIm ligand is similar to 5-methylimidazole (5-MeIm), a Cβ truncated model for the His ligand in myoglobin. SH^- was used widely to model axial Cys ligand of cytochrome P450 in previous studies.[1a,c] As seen from Table 1, both $\Delta G^{\ddagger}$ and ΔG° values for Fe(Por)(CPh_2)(MeIm) (**9**) and Fe(Por)(CPh_2)(SH^-) (**10**) are significantly larger than those for **4**, the IPC without corresponding axial ligands. Since EDA was used in experimental biocatalytic carbene transfers,[33a−d] the formation pathways for Fe(Por)($CHCO_2Et$)(5-MeIm) (**11**) and Fe(Por)($CHCO_2Et$)(SH^-) (**12**) were also studied. As seen from Figure 2C, comparing **9** with **11** and **10** with **12**, respectively, $\Delta G^{\ddagger}$ is decreased, while ΔG° is increased. This trend is the same as found with the comparison between **4** and **3**, the IPCs without corresponding axial ligands, which is due to carbene substituent effect studied above. Based on results for **9**−**12**, the His-like axial ligand greatly enhances IPC formation more than the Cys-like ligand, which may help understand the preferential use of His vs Cys in experimental studies of biocatalysts for carbene transfers.[33d] This could be due to stronger *trans* effect of the negatively charged Cys than the neutral His. Together with the biscarbene formation profiles studied above, all these data show that axial ligand makes IPC formation kinetically more difficult, which is consistent with the significantly reduced Q_{CT} and significantly elongated R^{TS}_{FeC} (Table 1). These data are consistent with experimental endeavors in this area: (1) Heme model Fe(TPFPP)(CPh_2)(MeIm) was not directly synthesized from the diazo precursor as with other IPCs with no axial ligands but was generated from IPC Fe(TPFPP)(CPh_2) with MeIm,[13] and no IPCs similar to **10** with an extremely high barrier were

DOI: 10.1021/jacs.5b03437
J. Am. Chem. Soc. 2015, 137, 7560−7563

reported experimentally. (2) For heme proteins, a wide range of mutations around the active site was carried out to achieve reasonable reactivities.[33a−d] Another interesting feature is that, in the biocatalytic IPC formation from EDA, there is a stable **Int** in the pathway (Figure 2C). In particular in the case of His ligand, it only needs 5.32 kcal/mol to form the **Int**. Since the experimental catalyst loading with respect to EDA is 0.2 mol%,[33a,c] the large excess of EDA can effectively improve the yield of **Int**. The $\Delta G^{\ddagger}$ from **Int** for the formation of **11** is only 16.29 kcal/mol, similar to those of **1** and **4**, formed by room temperature synthesis.[13] The effective ΔG° from **Int** is now thermodynamically favorable, −4.71 kcal/mol. These data further support the excellent role of His ligand in experimental biocatalytic carbene transfer reactions.[33c,d]

Overall, this work provides the first systematic investigation of the effects of carbene binding mode, carbene substituent, porphyrin substituent, and protein axial ligand on IPC formation. Results not only are consistent with available experimental data but also offer a number of unprecedented insights into the electronic, steric, and H-bonding effects of various structural factors on IPC formation. Given that iron is the least expensive and most abundant transition metal for catalysis and iron porphyrins/heme proteins are biocompatible catalysts, these first-time results will greatly facilitate future sustainable chemical catalysis and biocatalysis.

■ ASSOCIATED CONTENT

Supporting Information

Computational details, coordinates of optimized structures and their absolute energies, and the ChemDraw and 3D optimized structures of the 12 IPC complexes studied in this work. The Supporting Information is available free of charge on the ACS Publications website at DOI: 10.1021/jacs.5b03437.

■ AUTHOR INFORMATION

Corresponding Author

*yong.zhang@stevens.edu

Notes

The authors declare no competing financial interest.

■ ACKNOWLEDGMENTS

This work was supported by NSF grant CHE-1300912 and NIH grant GM085774 to Y.Z.

■ REFERENCES

(1) (a) Meunier, B.; de Visser, S. P.; Shaik, S. *Chem. Rev.* **2004**, *104*, 3947. (b) Bernhardt, R. *J. Biotechnol.* **2006**, *124*, 128. (c) de Visser, S. P.; Kumar, D.; Cohen, S.; Shacham, R.; Shaik, S. *J. Am. Chem. Soc.* **2004**, *126*, 8362. (d) Irigaray, P.; Belpomme, D. *Carcinogenesis* **2010**, *31*, 135.

(2) Che, C.-M.; Lo, V. K.-Y.; Zhou, C.-Y.; Huang, J.-S. *Chem. Soc. Rev.* **2011**, *40*, 1950.

(3) Che, C.-M.; Zhou, C.-Y.; Wong, E. L.-M. *Top. Organomet. Chem.* **2011**, *33*, 111.

(4) Morandi, B.; Carreira, E. M. *Science* **2012**, *335*, 1471.

(5) Maxwell, J. L.; Brown, K. C.; Bartley, D. W.; Kodadek, T. *Science* **1992**, *256*, 1544.

(6) Reddy, A. R.; Zhou, C.-Y.; Guo, Z.; Wei, J.; Che, C.-M. *Angew. Chem., Int. Ed.* **2014**, *53*, 14175.

(7) Xu, X.; Lu, H.; Ruppel, J. V.; Cui, X.; de Mesa, S. L.; Wojtas, L.; Zhang, X. P. *J. Am. Chem. Soc.* **2011**, *133*, 15292.

(8) Lu, H.; Dzik, W. I.; Xu, X.; Wojtas, L.; de Bruin, B.; Zhang, X. P. *J. Am. Chem. Soc.* **2011**, *133*, 8518.

(9) Dzik, W. I.; Xu, X.; Zhang, X. P.; Reek, J. N. H.; de Bruin, B. *J. Am. Chem. Soc.* **2010**, *132*, 10891.

(10) Ho, C.-M.; Zhang, J.-L.; Zhou, C.-Y.; Chan, O.-Y.; Yan, J. J.; Zhang, F.-Y.; Huang, J.-S.; Che, C.-M. *J. Am. Chem. Soc.* **2010**, *132*, 1886.

(11) Zhu, S.; Perman, J. A.; Zhang, X. P. *Angew. Chem., Int. Ed.* **2008**, *47*, 8460.

(12) Zhu, S.; Ruppel, J. V.; Lu, H.; Wojtas, L.; Zhang, X. P. *J. Am. Chem. Soc.* **2008**, *130*, 5042.

(13) Li, Y.; Huang, J. S.; Zhou, Z. Y.; Che, C. M.; You, X. Z. *J. Am. Chem. Soc.* **2002**, *124*, 13185.

(14) Thu, H. Y.; Tong, G. S. M.; Huang, J. S.; Chan, S. L. F.; Deng, Q. H.; Che, C. M. *Angew. Chem., Int. Ed.* **2008**, *47*, 9747.

(15) Mbuvi, H. A.; Woo, L. K. *Organometallics* **2008**, *27*, 637.

(16) Wang, J.-C.; Xu, Z.-J.; Guo, Z.; Deng, Q.-H.; Zhou, C.-Y.; Wan, X.-L.; Che, C.-M. *Chem. Commun.* **2012**, *48*, 4299.

(17) Li, Y.; Huang, J. S.; Zhou, Z. Y.; Che, C. M. *J. Am. Chem. Soc.* **2001**, *123*, 4843.

(18) Chen, Y.; Huang, L. Y.; Zhang, X. P. *Org. Lett.* **2003**, *5*, 2493.

(19) Baumann, L. K.; Mbuvi, H. M.; Du, G.; Woo, L. K. *Organometallics* **2007**, *26*, 3995.

(20) Che, C. M.; Huang, J. S.; Lee, F. W.; Li, Y.; Lai, T. S.; Kwong, H. L.; Teng, P. F.; Lee, W. S.; Lo, W. C.; Peng, S. M.; Zhou, Z. Y. *J. Am. Chem. Soc.* **2001**, *123*, 4119.

(21) Wolf, J. R.; Hamaker, C. G.; Djukic, J. P.; Kodadek, T.; Woo, L. K. *J. Am. Chem. Soc.* **1995**, *117*, 9194.

(22) Lai, T. S.; Chan, F. Y.; So, P. K.; Ma, D. L.; Wong, K. Y.; Che, C. M. *Dalton Trans.* **2006**, 4845.

(23) Hamaker, C. G.; Mirafzal, G. A.; Woo, L. K. *Organometallics* **2001**, *20*, 5171.

(24) Chen, Y.; Zhang, X. P. *J. Org. Chem.* **2007**, *72*, 5931.

(25) Chen, Y.; Huang, L. Y.; Ranade, M. A.; Zhang, X. P. *J. Org. Chem.* **2003**, *68*, 3714.

(26) Chen, Y.; Ruppel, J. V.; Zhang, X. P. *J. Am. Chem. Soc.* **2007**, *129*, 12074.

(27) Anding, B. J.; Ellern, A.; Woo, L. K. *Organometallics* **2012**, *31*, 3628.

(28) Callot, H. J.; Metz, F.; Piechocki, C. *Tetrahedron* **1982**, *38*, 2365.

(29) Smith, D. A.; Reynolds, D. N.; Woo, L. K. *J. Am. Chem. Soc.* **1993**, *115*, 2511.

(30) Smith, D. A.; Woo, L. K. *Organometallics* **1992**, *11*, 2344.

(31) Mansuy, D.; Lange, M.; Chottard, J. C.; Guerin, P.; Morliere, P.; Brault, D.; Rougee, M. *J. Chem. Soc., Chem. Commun.* **1977**, 648.

(32) (a) Simonneaux, G.; Le Maux, P. *Top. Organomet. Chem.* **2006**, 83. (b) Tolando, R.; Ferrara, R.; Eldirdiri, N. I.; Albores, A.; King, L. J.; Manno, M. *Xenobiotica* **1996**, *26*, 425. (c) Mansuy, D.; Battioni, J. P.; Chottard, J. C.; Ullrich, V. *J. Am. Chem. Soc.* **1979**, *101*, 3971. (d) Groves, J. T.; Avaria-Neisser, G. E.; Fish, K. M.; Imachi, M.; Kuczkowski, R. L. *J. Am. Chem. Soc.* **1986**, *108*, 3837. (e) Lafite, P.; Dijols, S.; Zeldin, D. C.; Dansette, P. M.; Mansuy, D. *Arch. Biochem. Biophys.* **2007**, *464*, 155. (f) Taxak, N.; Patel, B.; Bharatam, P. V. *Inorg. Chem.* **2013**, *52*, 5097.

(33) (a) Coehlo, P. S.; Brustad, E. M.; Kannan, A.; Arnold, F. H. *Science* **2013**, *339*, 307. (b) Coehlo, P. S.; Wang, Z. J.; Ener, M. E.; Baril, S. A.; Kannan, A.; Arnold, F. H.; Brustad, E. M. *Nat. Chem. Biol.* **2013**, *9*, 485. (c) Bordeaux, M.; Tyagi, V.; Fasan, R. *Angew. Chem., Int. Ed.* **2015**, *54*, 1744. (d) Wang, Z. J.; Renata, H.; Peck, N. E.; Farwell, C. C.; Coehlo, P. S.; Arnold, F. H. *Angew. Chem., Int. Ed.* **2014**, *53*, 6810. (e) Sreenilayam, G.; Fasan, R. *Chem. Commun.* **2015**, *51*, 1532.

(34) Nakamura, E.; Yoshikai, N.; Yamanaka, M. *J. Am. Chem. Soc.* **2002**, *124*, 7181.

(35) Chai, J.-D.; Head-Gordon, M. *Phys. Chem. Chem. Phys.* **2008**, *10*, 6615.

(36) Yang, K.; Zheng, J.; Zhao, Y.; Truhlar, D. G. *J. Chem. Phys.* **2010**, *132*, 164117.

(37) Khade, R. L.; Fan, W.; Ling, Y.; Yang, L.; Oldfield, E.; Zhang, Y. *Angew. Chem., Int. Ed.* **2014**, *53*, 7574.

(38) (a) Mansuy, D.; Battioni, J. P.; Lavallee, D. K.; Fischer, J.; Weiss, R. *Inorg. Chem.* **1988**, *27*, 1052. (b) Mansuy, D.; Lange, M.; Chottard, J. C.; Bartoli, J. F.; Chevrier, B.; Weiss, R. *Angew. Chem., Int. Ed.* **1978**, *17*, 781.

DOI: 10.1021/jacs.5b03437
J. Am. Chem. Soc. 2015, 137, 7560−7563